



Published in final edited form as:

Cell Rep. 2015 March 17; 10(10): 1692–1707. doi:10.1016/j.celrep.2015.02.027.

YAP inhibition restores hepatocyte differentiation in advanced HCC leading to tumor regression

Julien Fitamant^{1,2,4}, Filippos Kottakis^{1,2,4}, Samira Benhamouche^{1,5,6}, Helen S. Tian^{1,2}, Nicolas Chuvin^{1,2}, Christine A. Parachoniak^{1,2,4}, Julia M. Nagle^{1,2}, Rushika M. Perera^{1,2,4}, Marjorie Lapouge^{1,2}, Vikram Deshpande^{1,5}, Andrew X. Zhu^{1,4}, Albert Lai⁷, Bosun Min⁷, Yujin Hoshida⁸, Joseph Avruch^{3,4,12}, Daniela Sia^{8,9}, Genís Campreciós⁸, Andrea I. McClatchey^{1,5}, Josep M. Llovet^{8,10,11}, David Morrissey⁷, Lakshmi Raj⁷, and Nabeel Bardeesy^{1,2,4,12}

¹Cancer Center, Massachusetts General Hospital, 185 Cambridge Street, Boston, MA 02114, USA

²Center for Regenerative Medicine, Massachusetts General Hospital, 185 Cambridge Street, Boston, MA 02114, USA

³Department of Molecular Biology, Massachusetts General Hospital, 185 Cambridge Street, Boston, MA 02114, USA

⁴Department of Medicine, Harvard Medical School, Boston, MA 02114

⁵Department of Pathology, Harvard Medical School, Boston, MA 02114

⁶Inserm U1053, University of Bordeaux, 146 rue Leo Saignat, 33076 Bordeaux Cedex, France

⁷Novartis Institutes of Biomedical Research Inc. 250 Massachusetts Avenue, Cambridge, MA 02139 U.S.A

⁸Liver Cancer Program, Tisch Cancer Institute, Division of Liver Diseases, Department of Medicine, Icahn School of Medicine at Mount Sinai, New York, NY 10029, USA

⁹Gastrointestinal Surgery and Liver Transplantation Unit, National Cancer Institute, Milan 20133, Italy

¹⁰HCC Translational Research Laboratory, BCLC Group, Liver Unit, IDIBAPS, Hospital Clínic, CIBERehd, Universitat de Barcelona, Catalonia, Spain

¹²Corresponding Author: Bardeesy.Nabeel@mgh.harvard.edu; Phone: 617-643-2579; Fax: 617-643-3170, Avruch@molbio.mgh.harvard.edu; Phone: 617-643-6911; 617-726-5649.

ACCESSION NUMBERS

The NCBI GEO accession number for the data reported in this paper is pending

AUTHOR CONTRIBUTIONS

J.F., S.B., L.R. and N.B. designed experiments. J.F. performed experiments with the assistance of F.K., S.B., H.S.T., N.C., C.A.P., J.M.N., R.M.P., M.L., B.M. and G.C.

J.F., F.K., S.B., V.D., A.X.Z., A.L., Y.H., J.A., D.S., A.I.M., J.M.L., D.M., L.R. and N.B. analyzed the data. F.K. and S.B. contributed equally. J.F. and N.B. wrote the manuscript.

Publisher's Disclaimer: This is a PDF file of an unedited manuscript that has been accepted for publication. As a service to our customers we are providing this early version of the manuscript. The manuscript will undergo copyediting, typesetting, and review of the resulting proof before it is published in its final citable form. Please note that during the production process errors may be discovered which could affect the content, and all legal disclaimers that apply to the journal pertain.

¹¹Institució Catalana de Recerca i Estudis Avançats (ICREA), Barcelona, Catalonia, Spain

SUMMARY

Defective Hippo/YAP signaling in the liver results in tissue overgrowth and development of hepatocellular carcinoma (HCC). Here, we uncover mechanisms of YAP-mediated hepatocyte reprogramming and HCC pathogenesis. YAP functions as a rheostat maintaining metabolic specialization, differentiation and quiescence within the hepatocyte compartment. Increased or decreased YAP activity reprograms subsets of hepatocytes to different fates associated with deregulation of the HNF4A, CTNNB1, and E2F transcriptional programs controlling hepatocyte quiescence and differentiation. Importantly, treatment with siRNA-lipid nanoparticles (siRNA-LNPs) targeting YAP restores hepatocyte differentiation and causes pronounced tumor regression in a genetically engineered mouse HCC model. Furthermore, YAP targets are enriched in an aggressive human HCC subtype characterized by a proliferative signature and absence of *CTNNB1* mutations. Thus, our work reveals Hippo signaling as a key regulator of positional identity of hepatocytes, supports targeting YAP using siRNA-LNPs as a paradigm of differentiation-based therapy, and identifies an HCC subtype potentially responsive to this approach.

Keywords

Hippo pathway; hepatocellular carcinoma; differentiation therapy; siRNA lipid nanoparticles; YAP; liver differentiation; liver zonation

Introduction

Hepatocellular carcinoma (HCC) is the second most common cause of cancer-related death worldwide, and the incidence is increasing in the United States (El-Serag, 2011; Forner et al., 2012). Curative resection or transplantation is only possible in ~30% of patients, and for advanced HCC, the multi-kinase inhibitor, sorafenib, remains the only approved agent with modest survival benefits (Cheng et al., 2009; Llovet et al., 2008). Genomic studies have classified HCC into subsets with distinct molecular and clinical features (Chiang et al., 2008; Guichard et al., 2012; Hoshida et al., 2009; Lachenmayer et al., 2012). Activating *CTNNB1* mutations are the most common oncogenic drivers, present in ~30% of tumors, and define an HCC subtype characterized by a hepatocyte-like gene expression signature, well-differentiated histology, and improved survival. The other recurrent genetic alterations in HCC involve tumor suppressor inactivation (Fujimoto et al., 2012; Guichard et al., 2012) and have not pointed to readily targetable vulnerabilities. Thus, there is a need to more fully discern biologically distinct HCC subtypes and to identify therapeutic targets.

Hippo signaling is an important tumor suppressor mechanism in multiple tissues including the liver (Harvey et al., 2013; Mo et al., 2014). The core of the pathway involves a kinase cascade with the homologous MST1 and MST2 (STK3, STK4) proteins as upstream kinases that subsequently activate the LATS1/LATS2 kinases (Yu and Guan, 2013). Signaling inputs include G-protein coupled receptors, Rho GTPases, AMPK, and polarity complex proteins including NF2, AMOT, and α -CATENIN, which link Hippo activity to a variety of cues,

including cell contact, mitotic failure, nutrients and growth factors (Ganem et al., 2014; Yu and Guan, 2013). Major downstream targets are the transcriptional co-activators, YAP and TAZ, which are phosphorylated by LATS1/LATS2, leading to their cytoplasmic retention and degradation. YAP and TAZ promote growth, survival and/or stem cell-like phenotypes in many cellular contexts (Mo et al., 2014), although the key mediators of these processes are not clearly established.

In the adult mouse liver, inactivation of *Mst1/Mst2*, *Sav1* or *Nf2*, or ectopic expression of *Yap* all result in expansion of atypical ductal cells (ADCs, or “oval cells”), liver enlargement and progression to HCC or mixed HCC/cholangiocarcinoma; *Mst1/Mst2* KO or *Yap* overexpression also cause hepatocyte overproliferation (Camargo et al., 2007; Dong et al., 2007; Lee et al., 2010; Lu et al., 2010; Yimlamai et al., 2014; Zender et al., 2006; Zhou et al., 2009). Lineage tracing in *Yap* transgenic and *Nf2* KO livers indicate that the ADCs are derived from de-differentiation of hepatocytes (Yimlamai et al., 2014), consistent with emerging data demonstrating plasticity of these cells (Schaub et al., 2014; Yanger et al., 2014), and pointing to important functions of Hippo/YAP in controlling liver cell fate. Consistent with a role for activated YAP in human HCC, ~50% of these tumors exhibit nuclear YAP staining, and nuclear YAP levels correlate with decreased survival after resection (Tschaharganeh et al., 2013; Xu et al., 2009).

Here we sought to explore the role of YAP in HCC progression and maintenance in order to define its downstream oncogenic program, assess its potential as a therapeutic target, and establish biomarkers identifying the subsets of HCC where YAP targeting may be beneficial. By using genetic approaches and siRNA-lipid nanoparticle (siRNA-LNP) technology in genetically engineered mouse (GEM) models, we demonstrate that activation of endogenous YAP perturbs hepatocyte differentiation and maintains this state in advanced tumors. Correspondingly, YAP silencing in HCC restores hepatocyte differentiation and leads to tumor regression; this offers proof-of-concept that differentiation therapy has potential as a treatment strategy in an epithelial tumor. Moreover, the significant responses induced by siYAP-LNPs support ongoing clinical development of this therapeutic modality. Finally, our work shows that an aggressive subtype of human HCC — enriched for cell cycle gene expression and lacking *CTNNB1* mutations — exhibits a YAP activation signature, pointing to biomarkers to guide the deployment of YAP-directed therapies in clinical trials.

Results

Role of YAP downstream of MST1/MST2 in the control of hepatocyte identity

To begin to explore the relationship between Hippo pathway activity and liver cell differentiation, we examined Yap expression in normal mouse liver. The bile ducts showed strong nuclear YAP staining (Fig. 1A,B), consistent with prior observations (Yimlamai et al., 2014). We also observed a graded staining pattern in the hepatocyte compartment, with the periportal hepatocytes (adjacent to the bile duct) showing readily detectable Yap nuclear and cytoplasmic localization, and with pericentral hepatocytes (adjacent to the central vein) showing clear nuclear exclusion. SOX9 — like YAP, a marker of the bile ducts and liver cell plasticity (Antoniou et al., 2009; Shin et al., 2011; Yanger et al., 2013) — exhibited a similar expression pattern in hepatocytes along the porto-central axis (Fig. 1A, S1A). This staining

gradient is suggestive of a role for YAP in the zonation of hepatocytes, which have specialized metabolic functions depending on their position in the liver lobule (Jungermann and Katz, 1989). The zonation program is thought to be governed by the interplay of the HNF4A and WNT/ β -CATENIN pathways and is characterized by strict boundaries of expression of key metabolic genes in the pericentral region and periportal regions (e.g. glutamine synthase and glutaminase 2, respectively) (Benhamouche et al., 2006; Gougelet et al., 2014; Torre et al., 2011).

To study the impact of Hippo pathway modulation on liver cell identity and proliferation, we generated mice with liver-specific *Mst1/Mst2* double-knockout (DKO), *Yap* deletion (*Yap* KO), and DKO combined with hemizygous or homozygous *Yap* deletion (designated DKO *Yap*^{+/-} and TKO (triple-knockout) mice, respectively) via crosses of floxed strains to *Albumin-Cre* mice. Necropsy at 7 weeks revealed that DKO mice had massive liver overgrowth and high levels of hepatocyte proliferation, associated with upregulation of nuclear and total Yap levels throughout the hepatocyte compartment and marked expansion of SOX9⁺ and SOX9⁻ ADCs in the periportal region (Fig. 1C, S1B,C), as previously reported in other Hippo pathway mutant mouse models (Benhamouche et al., 2010; Lee et al., 2010; Lu et al., 2010; Yimlamai et al., 2014). In addition, DKO animals exhibited a striking loss of hepatocyte zonation as reflected by decreased pericentral expression of glutamine synthase (GS) and ornithine aminotransferase (OAT) (Fig. 1C,D, S1D). Each abnormality was rescued in DKO *Yap*^{+/-} and TKO mice, although the latter exhibited biliary defects, regional hepatocyte necrosis, cholestasis, fibrosis and swelling of the tissue as observed in *Yap* KO livers (Zhang et al., 2010). Notably, in *Yap* KO mice, we found that there was expansion of the GS-positive domain, whereby several layers of hepatocytes surrounding the central vein as well as scattered cells throughout the lobule showed aberrant induction of GS (Fig. 1D). These findings link aberrantly activated YAP to hepatocyte reprogramming downstream of MST1/MST2 and reveal an unexpected role of basal YAP function in maintenance of hepatocyte zonation.

Despite the ongoing expansion of ADCs, proliferating cells with hepatocyte morphology persist in the DKO liver and exhibit a higher frequency of PCNA staining than adjacent ADCs (Fig. S1C). Together the data imply that the response of hepatocytes to activation of endogenous YAP is distinct depending on their zonal location, creating a highly proliferative population of dedifferentiated, (GS-negative) pericentral hepatocytes as well as an expanded pool of ADCs emerging from periportal hepatocytes.

Acute deregulation of the Hippo pathway overrides hepatocyte zonation

These phenotypes were recapitulated in the setting of acute deregulation of the Hippo pathway using intravenous injection of Cre adenovirus to conditionally delete *Mst1/Mst2* and *Yap* in adult hepatocytes (designated as DKO^{Ad}, TKO^{Ad} and *Yap* KO^{Ad} models). Examination at 2 weeks post-injection revealed that DKO^{Ad} mice had increased hepatocyte proliferation, ADC expansion, and reduced pericentral GS expression compared to WT^{Ad} livers (Fig. 2A–C). These changes were rescued by *Yap* ablation (TKO^{Ad} and DKO *Yap*^{+/-}–^{Ad} models) and moreover, *Yap* KO^{Ad} mice exhibited expansion of the GS-positive domain (10.1 \pm 0.5% of hepatocytes were GS⁺ in WT^{Ad} livers, versus 16.0 \pm 0.9% in *Yap* KO^{Ad},

and 8.0+/-0.5% in DKO^{Ad}) (Fig. 2C and see **Methods**). Thus, YAP serves as a rheostat for maintenance of quiescence and identity in adult hepatocytes. In particular, activation of YAP overrides the pericentral zonation program and also directs periportal hepatocytes to dedifferentiate to ADCs, whereas basal levels of Yap are required to prevent the aberrant induction of a pericentral phenotype in multiple layers of hepatocytes surrounding the central vein.

We conducted gene expression profiling at day 8 following Ad-Cre administration to determine the early transcriptional changes provoked by *Mst1/Mst2* inactivation (WT^{Ad} versus DKO^{Ad}). Gene Set Enrichment Analysis (GSEA) revealed that acute *Mst1/Mst2* DKO caused potent inactivation of the hepatocyte differentiation program, with downregulation of hundreds of hepatocyte-specific genes (Fig. 2D). Accordingly, the set of downregulated genes was highly enriched for established targets of the master regulators of hepatocyte identity, HNF4A and FOXA2. Conversely, there was upregulation of cell proliferation signatures enriched for E2F target genes (Fig. 2E). Experimentally determined binding sites for TEAD/TEF-1 were significantly enriched in the promoter elements of the differentially expressed genes ($p < 2.0 \times 10^{-14}$) as was the consensus TEAD/TEF1 binding motif (Fig. S2A), consistent with TEAD family proteins being the key partners for YAP in the liver (Liu-Chittenden et al., 2012). We identified candidate direct YAP targets by integrating the expression analysis and chromatin immunoprecipitation data for TEAD binding in hepatic cells (HepG2 cells, ENCODE database)(Fig. S2B, Table S1). This gene set was highly enriched for predicted targets of HNF4A and FOXA1, which are master regulators of hepatocyte differentiation that cooperatively regulate many common targets (Fig. S2B)(Alder et al., 2014; Bochkis et al., 2012; Li et al., 2012). Notably, YAP has been shown to act as a switch for enhancer occupancy of HNF4A and FOXA2 in the liver, preventing expression of mature hepatocyte genes and promoting expression of liver stem cell (hepatoblast) genes (Alder et al., 2014). Moreover, deletion of *Hnf4a* in the adult liver results in hepatocyte dedifferentiation and the emergence of SOX9+ ADCs (Saha et al., 2014; Walesky et al., 2013). These observations suggest a potential mechanism involving interplay between activated YAP and an HNF4A/FOXA2/FOXA1 module for the control of hepatocyte identity and quiescence in DKO mice.

Yap status dictates HCC cell differentiation phenotypes downstream of Hippo inactivation

We next sought to assess the effects of YAP deficiency on the tumor phenotype caused by *Mst1/Mst2* DKO (Lu et al., 2010; Zhou et al., 2009). To this end, mice were either necropsied at serial time points or monitored until signs of poor body condition necessitated euthanasia, which in all cases was due the presence of liver tumors. At 15 weeks, DKO mice had rampant ADC expansion, whereas DKO Yap^{+/-} and TKO livers showed only focal appearance of hepatocyte-like cells staining strongly for SOX9, but limited or no cells with ADC morphology (Fig. 3A). In addition, TKO and DKO Yap^{+/-} mice had a marked extension in survival as compared to DKO animals (48.1 and 59.4 weeks, versus 23.5 weeks, respectively), and had reduced tumor burden (TKO 11 tumors/mouse; DKO Yap^{+/-} 10 tumors/mouse, DKO 39 tumors/mouse) (Fig. 3B,C). Immunohistochemistry confirmed that TKO tumors lacked Yap expression indicating that they did not emerge from rare cells that escaped *Yap* deletion (Fig. 3E, **lower panel**). Thus, Yap has a central role in tumorigenesis in

the DKO model and even single copy *Yap* ablation greatly delays HCC progression. On the other hand, observations from TKO mice demonstrate that *Mst1/Mst2* inactivation can still ultimately drive liver tumorigenesis through a YAP-independent, albeit less potent, program.

Histopathologic analysis at end-stage revealed that the tumors in each genotype were invasive HCC (Fig. 3E). However, the groups expressed distinct sets of differentiation markers, with the DKO HCCs staining for SOX9 and lacking both GS and nuclear β -CATENIN, and the great majority of TKO and DKO Yap $^{+/-}$ tumors showing the opposite profile (Fig. 3D,E). The phenotypes caused by liver-specific inactivation of *Nf2*, which are partially due to YAP activation, overlap those in DKO mice (Benhamouche et al., 2010; Yin et al., 2013; Zhang et al., 2010). Examination of *Nf2* KO HCCs revealed heterogeneous YAP staining in sharply demarcated regions. Those with higher nuclear and cytoplasmic YAP expressed SOX9 and lacked GS, whereas those with lower levels of YAP staining showed a reciprocal pattern (Fig. S3A), again correlating YAP levels and markers of HCC differentiation state. Together, these findings suggest a link between YAP-dependent hepatocyte reprogramming and HCC initiation, and connect YAP activity to the specific malignant phenotype of the ensuing tumors.

Therapeutic efficacy of siRNA-lipid nanoparticles targeting YAP in advanced HCC

We next explored the functions of YAP in the clinically relevant setting of maintenance of established tumors. In this regard, the use of siRNA encapsulated into lipid nanoparticles (siLNPs) — which improves cellular uptake, stability and pharmacokinetics of the siRNA (Whitehead et al., 2009) — is an approach to YAP targeting with clinical potential. Primary HCC is a particularly plausible cancer context for siRNA-LNP use since the dual blood supply and fenestrated endothelium in the liver lead to high perfusion, which may facilitate siRNA-LNP delivery. To test this strategy, we developed protocols to monitor tumor development in the DKO^{Ad} model by ultrasound (US) imaging. Pilot studies with serial imaging followed by necropsy provided histologic verification that the lesions detected by US were invasive HCC (Fig. 4A). Subsequently, an additional cohort was imaged, and animals with comparable tumor burden were randomized to receive tail vein injections of siLNPs targeting YAP or Luciferase (Luc) control (Fig. 4B, also see **Methods**). Mice were euthanized after 4 and 9 days to assess the acute responses. qRT-PCR and IHC revealed progressive YAP knockdown by siYap-LNPs (Fig. 4C–E, S4A). At day 4, IHC showed that 45% of tumor nodules had partial or complete reduction in YAP protein (Fig. 4E, S4A) (defined as % of HCC cells within the nodule staining above background; see Fig. S4B and **Methods**), and by day 9 this figure increased to 73.5% of nodules (29.4% partial, 44.1% complete) (Fig. 4D,E). We also observed coordinate reduction in expression of *Ctgf*, an established YAP-TEAD target, as well as of a series of E2F targets (Fig. 4C).

Importantly, siYAP-LNP treatment resulted in a prominent decrease in tumor cell proliferation that was proportional to the degree of knockdown at both day 4 and 9, as determined by KI67 and PCNA staining (Fig. 4D,F, **S4A,B**). At day 9, 25.5 \pm 1.6% of HCC cells in siLuc-LNP treated controls stained for proliferation markers, whereas the rates in the siYAP-LNP treated group were 2.9 \pm 0.4% and 11.8 \pm 1.1% in nodules with complete or partial Yap knockdown, respectively (Fig. 4D,F). There was no evidence of apoptosis as

determined by cleaved caspase-3 staining (Fig. S4A). These findings were corroborated using a second siLNP targeting a different YAP sequence (siYAP-LNP#2; Fig. S4C) and reveal a critical function of YAP in the proliferation of advanced HCC in this model.

To identify the transcriptional program underlying YAP-mediated tumor maintenance, we conducted RNA-sequencing (RNA-seq) on siLuc- and siYAP-treated tumors following 9 days treatment. GSEA revealed that YAP silencing caused potent inactivation of the E2F/cell proliferation pathway (Fig. 4G, S4D *left panel*). Reciprocally, there was a pronounced induction of a hepatocyte differentiation signature (Fig. 4H *left panel*), including activation of program of specific pericentral hepatocyte markers (Fig. 4H *right panel*), and enrichment of predicted HNF4A targets (Fig. S4D *right panel*). We integrated the set of genes altered by siYAP-LNP treatment in HCCs with ChIP data for TEAD occupancy in liver cancer cells in order to identify candidate direct YAP/TEAD target genes in these tumors (see **Methods**). To gain further insight into transcriptional circuits, we then searched this YAP/TEAD signature for enrichment of known binding sites for other transcription factors using the ENCODE database (Fig. S4E, Table S2). In line with our observations in the DKO liver, the YAP/TEAD signature was greatly enriched for HNF4 and FOXA1 binding sites, which were ranked first and second among all transcription factors analyzed, consistent with the interplay between these factors in dictating the balance between tumor maintenance and hepatocyte differentiation (Fig. S4E).

Comparison of the day 4 and day 9 time points indicated that the differentiation markers were gradually induced. At day 4, multiple HCC nodules with patchy staining for GS and nuclear β -CATENIN were observed in siYAP-LNP treated mice, with positively stained regions correlating with areas of more complete YAP knockdown (Fig. S4F). By day 9, uniform staining for both markers was frequently observed, coordinated with loss of SOX9 (Fig. 4I). Thus, YAP inhibition in aggressive HCC causes rapid downregulation of the E2F cell cycle pathway and progressive induction of a hepatocyte differentiation program associated with upregulation of HNF4/FOXA2/FOXA1 targets and increased activity of the pericentral/ β -CATENIN program.

siYAP-LNPs induce a hepatocyte differentiation program in advanced HCC

Tumor-bearing mice were treated with siRNA-LNPs for 4 weeks and then euthanized to determine the durability of the response and uncover any gradual consequences for tumor phenotypes. Consistent with the profound anti-proliferative effects seen upon acute YAP knockdown, the siYAP-LNP-treated animals showed a dramatic reduction in tumor burden as compared to controls, with marked decreases in number of HCCs (9.9 vs 0.5) and in their total cross-sectional area ($9.2 \times 10^6 \mu\text{m}^2$ vs $0.75 \times 10^6 \mu\text{m}^2$) (Fig. 5A). Adjacent regions of liver tissue showed restoration of zonal GS expression and complete elimination of ADCs (Fig. 5B). Remarkably, siYAP-LNP treatment resulted in the replacement of virtually all of invasive HCCs by areas of cells resembling regenerative hepatocyte nodules; in comparison to the HCCs in control animals, these cells had lower nuclear-to-cytoplasmic ratio, lacked mitotic figures, and had a reduction in cell plate thickness (Fig. 5C). Correspondingly, these nodules had low proliferation rates and showed induction of GS and nuclear β -catenin (Fig.

5C,D). Thus, sustained YAP inhibition provoked a broad hepatocyte differentiation program in established tumors.

The rare remaining HCC foci in siYAP-LNP treated animals exhibited persistent YAP expression suggesting that resistance arose either from augmented YAP expression or altered uptake or activity of the siRNA-LNPs (Fig. S5A). Importantly, the treatment regimen was well tolerated, causing no weight loss or significant changes in liver function values, and slight inflammation in periportal areas that was fully resolved within 2–4 weeks following discontinuation of treatment (Fig. S5B–D). These data indicate a central function of YAP in HCC tumor maintenance in the DKO model and support the application of siLNPs targeting YAP to treat advanced HCC. In addition, these studies provide proof-of-concept for differentiation therapy as an oncologic approach in the context of an aggressive epithelial tumor.

YAP-mediated control of proliferative and hepatic differentiation programs in primary tumor cultures

We used a series of early passage HCC tumor cultures derived from independent DKO and TKO mice to examine *in vitro* the relationship between Yap activity and proliferation and differentiation pathways. Consistent with our *in vivo* data, DKO tumor cultures grew more rapidly than TKO cultures, and were characterized by higher expression of multiple E2F-regulated cell cycle genes and lower expression of a set of HNF4A targets involved in specialized hepatocyte functions (Fig. 6A,B). Likewise, YAP knockdown in DKO cells caused proliferative arrest without evidence of cell death, whereas TKO cells were unaffected, demonstrating the specificity of the RNAi (Fig. 6C, S6A). The YAP-depleted DKO cells exhibited reduced expression of E2F target genes and pronounced activation of the HNF4A gene signature (Fig. 6D). Reciprocally, forced expression of YAP promoted the proliferation of TKO cultures (referred to as TKO-Yap cells) whereas it either slowed or did not affect the proliferation DKO cells that already harbor high YAP levels (Fig. 6E and data not shown). The TKO-Yap cells showed a corresponding induction of E2F target and suppression of the HNF4A targets (Fig. 6F). Finally, we found that TKO-Yap cells were sensitized to the CDK4 inhibitor, PD-0332991, at concentrations that did not affect TKO-Control cells (Fig. 6G, S6B). Thus, the role of YAP in sustaining proliferation and blocking differentiation is recapitulated in cultured HCC cells and points to direct functional roles for YAP in activating E2F and suppressing HNF4A activity in these tumors.

YAP activation is associated with the proliferative, CTNNB1 wild type subclass of HCC in humans

Mutations in *CTNNB1* define a distinct subtype of HCC with less aggressive clinical features (Chiang et al., 2008). Since we observed an inverse correlation between YAP and β -CATENIN activity in the DKO HCC model, our data predict that YAP activation and *CTNNB1* mutations may be associated with different HCC subtypes. In this regard, it is notable that nuclear β -CATENIN staining—which is closely correlated with *CTNNB1* mutations—and nuclear YAP staining show a strong negative association in human HCC specimens (Tao et al., 2014). We sought to extend these data by using our YAP activity signature to identify HCC subtypes potentially driven by YAP. This signature of presumptive

direct YAP targets was derived by integrating the set of genes altered by siYAP-LNP treatment in HCCs with ChIP data for TEAD occupancy in liver cancer cells; see Fig. S4E and **Methods**). To this end, enrichment for the YAP activation signature was calculated for each of the 111 HCC patients included in our human cohort. Correspondingly, nearest template prediction (NTP) revealed that the YAP gene expression signature had a strong negative correlation with *CTNNB1* mutation signature in this set of human HCCs (Lachenmayer et al., 2012) (Fig. 7A). These findings were corroborated using three additional independent HCC classification systems (Fig. S7A–C). Moreover, patients positive for the YAP expression signature showed strong enrichment in the “Proliferation”, poor prognosis gene expression subtype of HCC (Fig. 7B, S7A) (Chiang et al., 2008). In addition, YAP levels showed close correlation with an E2F target gene/proliferation signature across both HCC cell lines and human specimens (Fig. S7D, E). Together, these data suggest that YAP specifically contributes to the growth of an aggressive *CTNNB1* WT subtype of human HCC and point to the potential therapeutic value in targeting YAP in these currently intractable tumors.

DISCUSSION

We have shown that siRNA-LNP-mediated inhibition of YAP is an effective therapeutic in a GEM model of advanced HCC. In response to YAP inactivation, tumor cells undergo rapid proliferative arrest and subsequently acquire features of hepatocyte differentiation. These findings demonstrate the potential of YAP as a drug target in HCC and suggest a paradigm for differentiation therapy for the treatment of this aggressive epithelial malignancy.

Whereas YAP activation can induce anti-apoptotic genes and enhance cell survival in multiple contexts including livers treated with FAS ligand (Camargo et al., 2007; Zhou et al., 2009), we found no evidence of cell death upon siYAP-LNP administration in our HCC model. Rather, there was inhibition of E2F target genes and pronounced reduction in cell proliferation followed by a gradual activation of a hepatocyte differentiation program, culminating in the morphologic differentiation of the HCCs into nodules resembling regenerative hepatocytes. Thus, YAP inhibition in advanced HCC results in a remarkable reversion of transformed cells toward a growth arrested and histopathologically benign phenotype.

Anti-cancer drug development has focused largely on the identification of agents that incite death of the tumor cells. An alternative approach is to attempt to instruct cancer cells to reactivate differentiation programs thereby abrogating self-renewal and replicative lifespan. To date, this approach has been used to great success in acute promyelocytic leukemia harboring the *PML/RARA* fusion gene whereby all-trans retinoic acid and arsenic trioxide induce terminal differentiation of the leukemic cells into mature granulocytes and block their self-renewal (de The and Chen, 2010). Whether adult epithelial malignancies retain a latent capacity to differentiate and whether distinct nodes in cell regulation can be identified as targets to restore this differentiation potential are key questions in the broader application of such strategies. Our work provides a proof-of-concept for this approach in an autochthonous model of aggressive HCC and identifies YAP as such a targetable node. Differentiated hepatocytes survive for an extended period of time, therefore it remains to be seen whether a

While Yap deletion delayed tumorigenesis in DKO mice, it did not completely prevent formation of HCC. Rather, DKO Yap^{+/-} and TKO animals all eventually developed invasive HCC. These data are consistent with MST1/MST2 acting to suppress HCC development through targets in addition to YAP. It is possible that TAZ — which is expressed in the HCCs and derivative cell lines (data not shown) — partially compensates for YAP inactivation in this context. Since YAP deficiency eliminated ADCs in TKO mice and resulted in a distinct tumor phenotype—well-differentiated histology, β -CATENIN and GS positive, and SOX9 negative (Fig. 3D, 7C), it appears that this secondary pathway does not fully recapitulate the broad reprogramming of hepatocyte differentiation induced by YAP.

The link between YAP activity and differentiation status in HCC appears to be relevant in the corresponding human tumors. Using the transcriptional alterations provoked by YaAP inactivation in our HCC model as a read-out for YAP activity, we find that the YAP signature is negatively correlated with the *CTNNB1* mutant subclass of HCC and positively correlated with the “proliferation” subclass (Fig. 7A,B, S7A–C). These data extend findings from IHC analysis showing inverse correlation between nuclear YAP and nuclear β -CATENIN (Tao et al., 2014), and point to a molecular subtype of HCC that may benefit from anti-YAP therapies.

Targeting YAP as a cancer therapy is particularly compelling due to the clear dosage dependence of its oncogenic activity. Approaches to inhibit YAP using small molecules and peptides have been described (Jiao et al., 2014; Liu-Chittenden et al., 2012). Our data suggest that there may be a clinical path forward using siYAP-LNPs to treat primary HCC. Importantly as a genetically-targeted therapy, siYAP-LNPs would be expected to have more specificity and lower toxicity than most small molecule inhibitors, and indeed, we observed mild and reversible side effects in our studies (Fig. S5B–D). Finally, siRNA-LNPs can readily be adapted to inhibit multiple targets, enabling development of combinatorial strategies.

EXPERIMENTAL PROCEDURES

Mouse models

Mice were housed in pathogen-free animal facilities at Massachusetts General Hospital (MGH). All experiments were conducted under protocol 2005N000148 approved by the Subcommittee on Research Animal Care at MGH. The following mouse strains were used: *Mst1*⁻, *Mst2*^{Flox}, *Yap*^{Flox} and *Albumin-Cre* (Postic and Magnuson, 2000; Schlegelmilch et al., 2011; Zhou et al., 2009). The *Albumin-Cre* transgene efficiently deletes floxed sequences in all liver lineages by 4–6 weeks of age. Mice were maintained on a mixed genetic background and each genotype was generated from intercrosses from the same colony. For Adeno-Cre studies, 5×10^9 pfu of CMV-Cre adenovirus resuspended in a final volume of 200 μ l PBS was injected in the tail vein of 6-week old mice. All mice included in the survival analysis were euthanized when criteria for disease burden were reached (including abdominal distension that impeded movement, loss of >15% of weight body weight, labored breathing and/or abnormal posture).

siLNP formulations

LNPs were formed by mixing equal volumes of lipids dissolved in alcohol (the lipid solution contains a cationic lipid, a helper lipid (cholesterol), a neutral lipid (DSPC) and a PEG lipid), with siRNA (dissolved in sodium citrate: sodium chloride buffer, pH 4.0) by an impinging jet process. Following an incubation period, the solution was concentrated and diafiltered by ultrafiltration process using membranes with molecular weight cutoff from 100 KD. The product was sterile filtered and stored at 4°C. The total siRNA was determined by anion exchange chromatography. The targeted sequences for Yap are 5'-TTAAGAAAGTATCTTTGACC-3' (siYap-LNP #1) and 5'-TTAAGAAAGGGATCGGAAC-3' (siYap-LNP #2). A formulation targeting luciferase (siLuc-LNP) was used as a control. Formulations were intravenously injected (via tail vein) at 3 mg/kg per injection every other day (for short term treatment, i.e. < 10 days treatment) or for three consecutive days with a resting period of 2 days between every round of treatment for long-term analysis.

Gene-set enrichment analysis

GSEA (<http://www.broadinstitute.org/gsea/index.jsp>) of the expression data was used to assess enrichment of gene signatures. Depending upon the data set, there were several different methods used to rank genes: In the siRNA-LNP studies, a pairwise GSEA was performed by creating ranked lists of genes using the log₂ ratio of siYAP-LNPs to siLuc-LNPs and p-values were obtained by permuting the gene set. For the identification of direct target genes (Fig. S2B and S4E), TEAD ChIP peaks for HEPG2 cells were downloaded from ENCODE (<http://genome.ucsc.edu/ENCODE/>) and TEAD-target lists were generated by associating genes to TEAD peaks using PeakAnalyzer (Salmon-Divon et al., 2010) with the “closest-TSS” routine. We defined YAP signatures by comparing the differentially regulated genes in D8 or D9 and TEAD-targets. For transcription factor enrichment analysis, the ENCODE ChIP-seq significance tool was utilized (Auerbach et al., 2013). In brief, YAP-TEAD lists for D8 or D9 were uploaded in the web interface (<http://encodeqt.simple-encode.org>) and transcription factor binding sites were detected in the region +5000 bp to -2500 bp relative to the TSS of each gene. Significance of enrichment of a transcription factor was calculated by the hypergeometric test and corrected for multiple testing using the Benjamini-Hochberg FDR.

Supplementary Material

Refer to Web version on PubMed Central for supplementary material.

Acknowledgments

We thank Bardeesy lab members as well as A. Kimmelman and W. Kim for helpful comments and F. Camargo for generously providing the Yap^{fl} mice. The authors are thankful to the Novartis siRNA formulation group for siLNPs preparation, K. Ross for bioinformatics assistance, and D. Zhou for initiation of the mouse cohort. This work was supported by grants from the NIH/NCI (R01CA136567 and P50CA127003 to N.B. and J.A.), NIH/NIDDK (R01DK099558 to Y.H.), and the TargetCancer Foundation (to N.B.). N.B. holds the Gallagher Chair in Gastrointestinal Cancer Research at Massachusetts General Hospital. N.B. and J.M.L. are members of the Waxman Institute without Walls. J.F and S.B are recipients of Long-term postdoctoral fellowships from EMBO and the International Human Frontiers Science Program, respectively, and both were supported by ECOR Fund for Medical Discovery Postdoctoral Fellowships. C.P. is recipient of a CIHR postdoctoral fellowship. J.M.L. and D.S. are

supported by the Asociación Española Contra el Cáncer. A.L., B.M., D.M., and L.R. are employees of Novartis, and J.M.L. is a consultant with Novartis. This work is dedicated to the bright memory of Rolande Fitamant (1959–2014).

References

- Alder O, Cullum R, Lee S, Kan AC, Wei W, Yi Y, Garside VC, Bilenky M, Griffith M, Morrissy AS, et al. 2014; Hippo Signaling Influences HNF4A and FOXA2 Enhancer Switching during Hepatocyte Differentiation. *Cell reports*. 9:261–271. [PubMed: 25263553]
- Antoniou A, Raynaud P, Cordi S, Zong Y, Tronche F, Stanger BZ, Jacquemin P, Pierreux CE, Clotman F, Lemaigre FP. 2009; Intrahepatic bile ducts develop according to a new mode of tubulogenesis regulated by the transcription factor SOX9. *Gastroenterology*. 136:2325–2333. [PubMed: 19403103]
- Auerbach RK, Chen B, Butte AJ. 2013; Relating genes to function: identifying enriched transcription factors using the ENCODE ChIP-Seq significance tool. *Bioinformatics*. 29:1922–1924. [PubMed: 23732275]
- Benhamouche S, Curto M, Saotome I, Gladden AB, Liu CH, Giovannini M, McClatchey AI. 2010; Nf2/Merlin controls progenitor homeostasis and tumorigenesis in the liver. *Genes Dev*. 24:1718–1730. [PubMed: 20675406]
- Benhamouche S, Decaens T, Godard C, Chambrey R, Rickman DS, Moinard C, Vasseur-Cognet M, Kuo CJ, Kahn A, Perret C, Colnot S. 2006; Apc tumor suppressor gene is the “zonation-keeper” of mouse liver. *Dev Cell*. 10:759–770. [PubMed: 16740478]
- Bochkis IM, Schug J, Ye DZ, Kurinna S, Stratton SA, Barton MC, Kaestner KH. 2012; Genome-wide location analysis reveals distinct transcriptional circuitry by paralogous regulators Foxa1 and Foxa2. *PLoS Genet*. 8:e1002770. [PubMed: 22737085]
- Bonzo JA, Ferry CH, Matsubara T, Kim JH, Gonzalez FJ. 2012; Suppression of hepatocyte proliferation by hepatocyte nuclear factor 4alpha in adult mice. *J Biol Chem*. 287:7345–7356. [PubMed: 22241473]
- Braeuning A, Ittrich C, Kohle C, Hailfinger S, Bonin M, Buchmann A, Schwarz M. 2006; Differential gene expression in periportal and perivenous mouse hepatocytes. *The FEBS journal*. 273:5051–5061. [PubMed: 17054714]
- Camargo FD, Gokhale S, Johnnidis JB, Fu D, Bell GW, Jaenisch R, Brummelkamp TR. 2007; YAP1 increases organ size and expands undifferentiated progenitor cells. *Current biology : CB*. 17:2054–2060. [PubMed: 17980593]
- Cheng AL, Kang YK, Chen Z, Tsao CJ, Qin S, Kim JS, Luo R, Feng J, Ye S, Yang TS, et al. 2009; Efficacy and safety of sorafenib in patients in the Asia-Pacific region with advanced hepatocellular carcinoma: a phase III randomised, double-blind, placebo-controlled trial. *The Lancet Oncology*. 10:25–34. [PubMed: 19095497]
- Chiang DY, Villanueva A, Hoshida Y, Peix J, Newell P, Minguez B, LeBlanc AC, Donovan DJ, Thung SN, Sole M, et al. 2008; Focal gains of VEGFA and molecular classification of hepatocellular carcinoma. *Cancer Res*. 68:6779–6788. [PubMed: 18701503]
- de The H, Chen Z. 2010; Acute promyelocytic leukaemia: novel insights into the mechanisms of cure. *Nature reviews Cancer*. 10:775–783. [PubMed: 20966922]
- Dong J, Feldmann G, Huang J, Wu S, Zhang N, Comerford SA, Gayyed MF, Anders RA, Maitra A, Pan D. 2007; Elucidation of a universal size-control mechanism in *Drosophila* and mammals. *Cell*. 130:1120–1133. [PubMed: 17889654]
- Ehmer U, Zmoos AF, Auerbach RK, Vaka D, Butte AJ, Kay MA, Sage J. 2014; Organ size control is dominant over Rb family inactivation to restrict proliferation in vivo. *Cell reports*. 8:371–381. [PubMed: 25017070]
- El-Serag HB. 2011; Hepatocellular carcinoma. *N Engl J Med*. 365:1118–1127. [PubMed: 21992124]
- Forner A, Llovet JM, Bruix J. 2012; Hepatocellular carcinoma. *Lancet*. 379:1245–1255. [PubMed: 22353262]
- Fujimoto A, Totoki Y, Abe T, Boroevich KA, Hosoda F, Nguyen HH, Aoki M, Hosono N, Kubo M, Miya F, et al. 2012; Whole-genome sequencing of liver cancers identifies etiological influences on

mutation patterns and recurrent mutations in chromatin regulators. *Nat Genet.* 44:760–764. [PubMed: 22634756]

- Ganem NJ, Cornils H, Chiu SY, O'Rourke KP, Arnaud J, Yimlamai D, They M, Camargo FD, Pellman D. 2014; Cytokinesis failure triggers hippo tumor suppressor pathway activation. *Cell.* 158:833–848. [PubMed: 25126788]
- Gougelet A, Torre C, Veber P, Sartor C, Bachelot L, Denechaud PD, Godard C, Moldes M, Burnol AF, Dubuquoy C, et al. 2014; T-cell factor 4 and beta-catenin chromatin occupancies pattern zonal liver metabolism in mice. *Hepatology.* 59:2344–2357. [PubMed: 24214913]
- Guichard C, Amaddeo G, Imbeaud S, Ladeiro Y, Pelletier L, Maad IB, Calderaro J, Bioulac-Sage P, Letexier M, Degos F, et al. 2012; Integrated analysis of somatic mutations and focal copy-number changes identifies key genes and pathways in hepatocellular carcinoma. *Nat Genet.* 44:694–698. [PubMed: 22561517]
- Harvey KF, Zhang X, Thomas DM. 2013; The Hippo pathway and human cancer. *Nature reviews Cancer.* 13:246–257. [PubMed: 23467301]
- Hoshida Y, Nijman SM, Kobayashi M, Chan JA, Brunet JP, Chiang DY, Villanueva A, Newell P, Ikeda K, Hashimoto M, et al. 2009; Integrative transcriptome analysis reveals common molecular subclasses of human hepatocellular carcinoma. *Cancer Res.* 69:7385–7392. [PubMed: 19723656]
- Jiao S, Wang H, Shi Z, Dong A, Zhang W, Song X, He F, Wang Y, Zhang Z, Wang W, et al. 2014; A peptide mimicking VGLL4 function acts as a YAP antagonist therapy against gastric cancer. *Cancer Cell.* 25:166–180. [PubMed: 24525233]
- Jungermann K, Katz N. 1989; Functional specialization of different hepatocyte populations. *Physiological reviews.* 69:708–764. [PubMed: 2664826]
- Lachenmayer A, Alsinet C, Savic R, Cabellos L, Toffanin S, Hoshida Y, Villanueva A, Minguez B, Newell P, Tsai HW, et al. 2012; Wnt-pathway activation in two molecular classes of hepatocellular carcinoma and experimental modulation by sorafenib. *Clinical cancer research : an official journal of the American Association for Cancer Research.* 18:4997–5007. [PubMed: 22811581]
- Lee KP, Lee JH, Kim TS, Kim TH, Park HD, Byun JS, Kim MC, Jeong WI, Calvisi DF, Kim JM, Lim DS. 2010; The Hippo-Salvador pathway restrains hepatic oval cell proliferation, liver size, and liver tumorigenesis. *Proc Natl Acad Sci U S A.* 107:8248–8253. [PubMed: 20404163]
- Li Z, Tuteja G, Schug J, Kaestner KH. 2012; Foxa1 and Foxa2 are essential for sexual dimorphism in liver cancer. *Cell.* 148:72–83. [PubMed: 22265403]
- Liu-Chittenden Y, Huang B, Shim JS, Chen Q, Lee SJ, Anders RA, Liu JO, Pan D. 2012; Genetic and pharmacological disruption of the TEAD-YAP complex suppresses the oncogenic activity of YAP. *Genes Dev.* 26:1300–1305. [PubMed: 22677547]
- Llovet JM, Ricci S, Mazzaferro V, Hilgard P, Gane E, Blanc JF, de Oliveira AC, Santoro A, Raoul JL, Forner A, et al. 2008; Sorafenib in advanced hepatocellular carcinoma. *N Engl J Med.* 359:378–390. [PubMed: 18650514]
- Lu L, Li Y, Kim SM, Bossuyt W, Liu P, Qiu Q, Wang Y, Halder G, Finegold MJ, Lee JS, Johnson RL. 2010; Hippo signaling is a potent in vivo growth and tumor suppressor pathway in the mammalian liver. *Proc Natl Acad Sci U S A.* 107:1437–1442. [PubMed: 20080689]
- Mo JS, Park HW, Guan KL. 2014; The Hippo signaling pathway in stem cell biology and cancer. *EMBO Rep.* 15:642–656. [PubMed: 24825474]
- Postic C, Magnuson MA. 2000; DNA excision in liver by an albumin-Cre transgene occurs progressively with age. *Genesis.* 26:149–150. [PubMed: 10686614]
- Saha SK, Parachoniak CA, Ghanta KS, Fitamant J, Ross KN, Najem MS, Gurumurthy S, Akbay EA, Sia D, Cornella H, et al. 2014; Mutant IDH inhibits HNF-4alpha to block hepatocyte differentiation and promote biliary cancer. *Nature.* 513:110–114. [PubMed: 25043045]
- Salmon-Divon M, Dvinge H, Tammoja K, Bertone P. 2010; PeakAnalyzer: genome-wide annotation of chromatin binding and modification loci. *BMC bioinformatics.* 11:415. [PubMed: 20691053]
- Schaub JR, Malato Y, Gormond C, Willenbring H. 2014; Evidence against a stem cell origin of new hepatocytes in a common mouse model of chronic liver injury. *Cell reports.* 8:933–939. [PubMed: 25131204]

- Schlegelmilch K, Mohseni M, Kirak O, Pruszk J, Rodriguez JR, Zhou D, Kreger BT, Vasioukhin V, Avruch J, Brummelkamp TR, Camargo FD. 2011; Yap1 acts downstream of alpha-catenin to control epidermal proliferation. *Cell*. 144:782–795. [PubMed: 21376238]
- Shin S, Walton G, Aoki R, Brondell K, Schug J, Fox A, Smirnova O, Dorrell C, Erker L, Chu AS, et al. 2011; Foxl1-Cre-marked adult hepatic progenitors have clonogenic and bilineage differentiation potential. *Genes Dev*. 25:1185–1192. [PubMed: 21632825]
- Tao J, Calvisi DF, Ranganathan S, Cigliano A, Zhou L, Singh S, Jiang L, Fan B, Terracciano L, Armeanu-Ebinger S, et al. 2014; Activation of beta-catenin and Yap1 in human hepatoblastoma and induction of hepatocarcinogenesis in mice. *Gastroenterology*. 147:690–701. [PubMed: 24837480]
- Torre C, Perret C, Colnot S. 2011; Transcription dynamics in a physiological process: beta-catenin signaling directs liver metabolic zonation. *The international journal of biochemistry & cell biology*. 43:271–278. [PubMed: 19914393]
- Tremblay AM, Missiaglia E, Galli GG, Hettmer S, Urcia R, Carrara M, Judson RN, Thway K, Nadal G, Selve JL, et al. 2014; The Hippo transducer YAP1 transforms activated satellite cells and is a potent effector of embryonal rhabdomyosarcoma formation. *Cancer Cell*. 26:273–287. [PubMed: 25087979]
- Tschaharganeh DF, Chen X, Latzko P, Malz M, Gaida MM, Felix K, Ladu S, Singer S, Pinna F, Gretz N, et al. 2013; Yes-associated protein up-regulates Jagged-1 and activates the Notch pathway in human hepatocellular carcinoma. *Gastroenterology*. 144:1530–1542. e1512. [PubMed: 23419361]
- Walesky C, Gunewardena S, Terwilliger EF, Edwards G, Borude P, Apte U. 2013; Hepatocyte-specific deletion of hepatocyte nuclear factor-4alpha in adult mice results in increased hepatocyte proliferation. *Am J Physiol Gastrointest Liver Physiol*. 304:G26–37. [PubMed: 23104559]
- Whitehead KA, Langer R, Anderson DG. 2009; Knocking down barriers: advances in siRNA delivery. *Nature reviews Drug discovery*. 8:129–138. [PubMed: 19180106]
- Xu MZ, Yao TJ, Lee NP, Ng IO, Chan YT, Zender L, Lowe SW, Poon RT, Luk JM. 2009; Yes-associated protein is an independent prognostic marker in hepatocellular carcinoma. *Cancer*. 115:4576–4585. [PubMed: 19551889]
- Yanger K, Knigin D, Zong Y, Maggs L, Gu G, Akiyama H, Pikarsky E, Stanger BZ. 2014; Adult hepatocytes are generated by self-duplication rather than stem cell differentiation. *Cell stem cell*. 15:340–349. [PubMed: 25130492]
- Yanger K, Zong Y, Maggs LR, Shapira SN, Maddipati R, Aiello NM, Thung SN, Wells RG, Greenbaum LE, Stanger BZ. 2013; Robust cellular reprogramming occurs spontaneously during liver regeneration. *Genes Dev*. 27:719–724. [PubMed: 23520387]
- Yimlamai D, Christodoulou C, Galli GG, Yanger K, Pepe-Mooney B, Gurung B, Shrestha K, Cahan P, Stanger BZ, Camargo FD. 2014; Hippo pathway activity influences liver cell fate. *Cell*. 157:1324–1338. [PubMed: 24906150]
- Yin F, Yu J, Zheng Y, Chen Q, Zhang N, Pan D. 2013; Spatial organization of Hippo signaling at the plasma membrane mediated by the tumor suppressor Merlin/NF2. *Cell*. 154:1342–1355. [PubMed: 24012335]
- Yu FX, Guan KL. 2013; The Hippo pathway: regulators and regulations. *Genes Dev*. 27:355–371. [PubMed: 23431053]
- Zender L, Spector MS, Xue W, Flemming P, Cordon-Cardo C, Silke J, Fan ST, Luk JM, Wigler M, Hannon GJ, et al. 2006; Identification and validation of oncogenes in liver cancer using an integrative oncogenomic approach. *Cell*. 125:1253–1267. [PubMed: 16814713]
- Zhang N, Bai H, David KK, Dong J, Zheng Y, Cai J, Giovannini M, Liu P, Anders RA, Pan D. 2010; The Merlin/NF2 tumor suppressor functions through the YAP oncoprotein to regulate tissue homeostasis in mammals. *Dev Cell*. 19:27–38. [PubMed: 20643348]
- Zhou D, Conrad C, Xia F, Park JS, Payer B, Yin Y, Lauwers GY, Thasler W, Lee JT, Avruch J, Bardeesy N. 2009; Mst1 and Mst2 maintain hepatocyte quiescence and suppress hepatocellular carcinoma development through inactivation of the Yap1 oncogene. *Cancer Cell*. 16:425–438. [PubMed: 19878874]

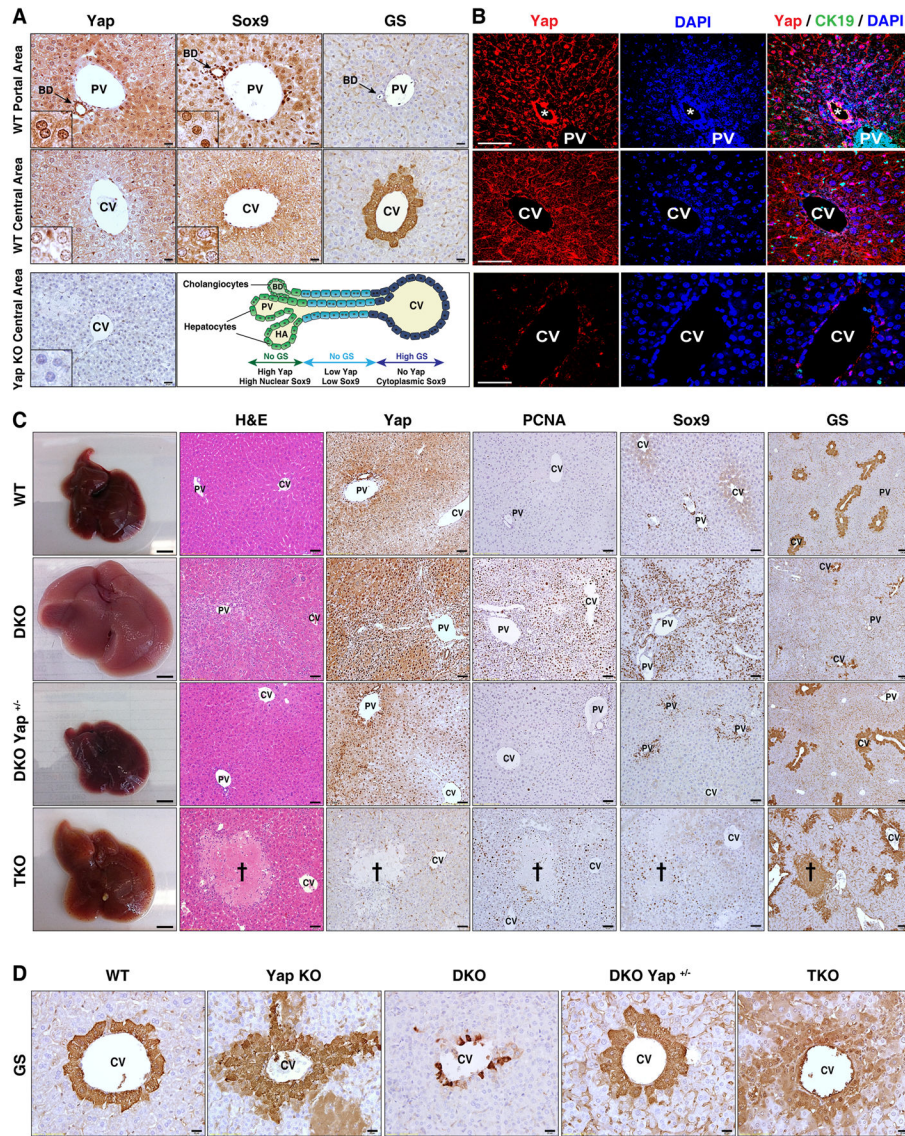


Figure 1. Hippo signaling is a rheostat controlling hepatocyte identity

A, B. Immunohistochemistry (**A**) and immunofluorescence (**B**) of mouse liver in the region of the portal vein (*top row*) and central vein (*middle row*) demonstrating nuclear and cytoplasmic YAP staining in bile ducts (arrow) and periportal hepatocytes, and absence of YAP in the first layer of pericentral hepatocytes. SOX9 shows nuclear staining in bile ducts and weaker nuclear staining in periportal hepatocytes, whereas it is excluded from the nucleus in pericentral hepatocytes. GS is a pericentral marker. CK19 is a biliary marker. The schematic representation of the porto-central axis indicates the territories of expression for YAP, SOX9 and GS. *Yap* KO liver (*bottom row*) is a negative control for YAP staining. Insets show magnified periportal or pericentral hepatocytes in (A). Bile duct is indicated by an asterisk in (B). Scale bars: 20µm (A) and 50µm (B).

C. Gross, histologic and IHC analysis of livers of the indicated genotypes (Albumin-Cre models). Cross: necrotic region in TKO. Scale bars: 5mm (gross), 50µm (H&E, YAP, PCNA, SOX9) and 100 µm (GS).

D. GS staining in pericentral regions. Scale bar: 20 μ m.
PV: Portal vein, CV: Central vein, BD: Bile duct, HA: Hepatic artery.
See also Figure S1.

Author Manuscript

Author Manuscript

Author Manuscript

Author Manuscript

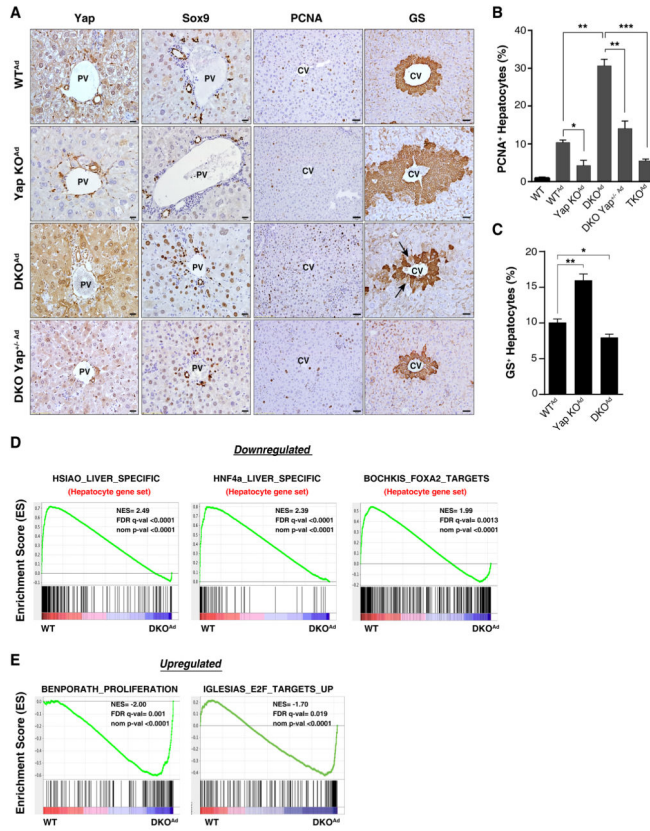


Figure 2. Acute effect of Hippo pathway modulation on hepatocyte identity

A–C. Mice were administered Cre adenovirus intravenously and livers were analyzed 2 weeks later by IHC for YAP, SOX9, PCNA and GS. The graphs quantify PCNA (**B**) and GS (**C**) staining. N= 3 mice in the WT, WT^{Ad}, Yap KO^{Ad}, TKO^{Ad} groups; 4 mice in the DKO Yap^{+/- Ad} group and 5 mice in the DKO^{Ad} group. Error bars indicate S.E.M. *p<0.05, **p<0.01, ***p<0.001, ****p<0.0001. Scale bars: 20µm (YAP, SOX9) and 50µm (PCNA, GS).

D, E. GSEA of mRNA expression data after acute deletion of *Mst1/Mst2* in liver. DKO and WT mice were administered Adeno-Cre and liver mRNA was isolated after 8 days. **D.** GSEA revealed rapid loss of a broad program of hepatocyte differentiation genes and of targets of the master hepatocyte regulators, HNF4A and FOXA2. **E)** GSEA showing strong induction of a proliferation gene signature including established E2F targets. Liver-derived gene sets are indicated in red. NES: Normalized enrichment score; FDR: False discovery rate. Gene sets are from the Molecular Signatures Database except (HNF4a_LIVER_SPECIFIC) which is a curated list of liver-specific HNF4A targets (Saha et al., 2014).

See also Figure S2 and Table S1.

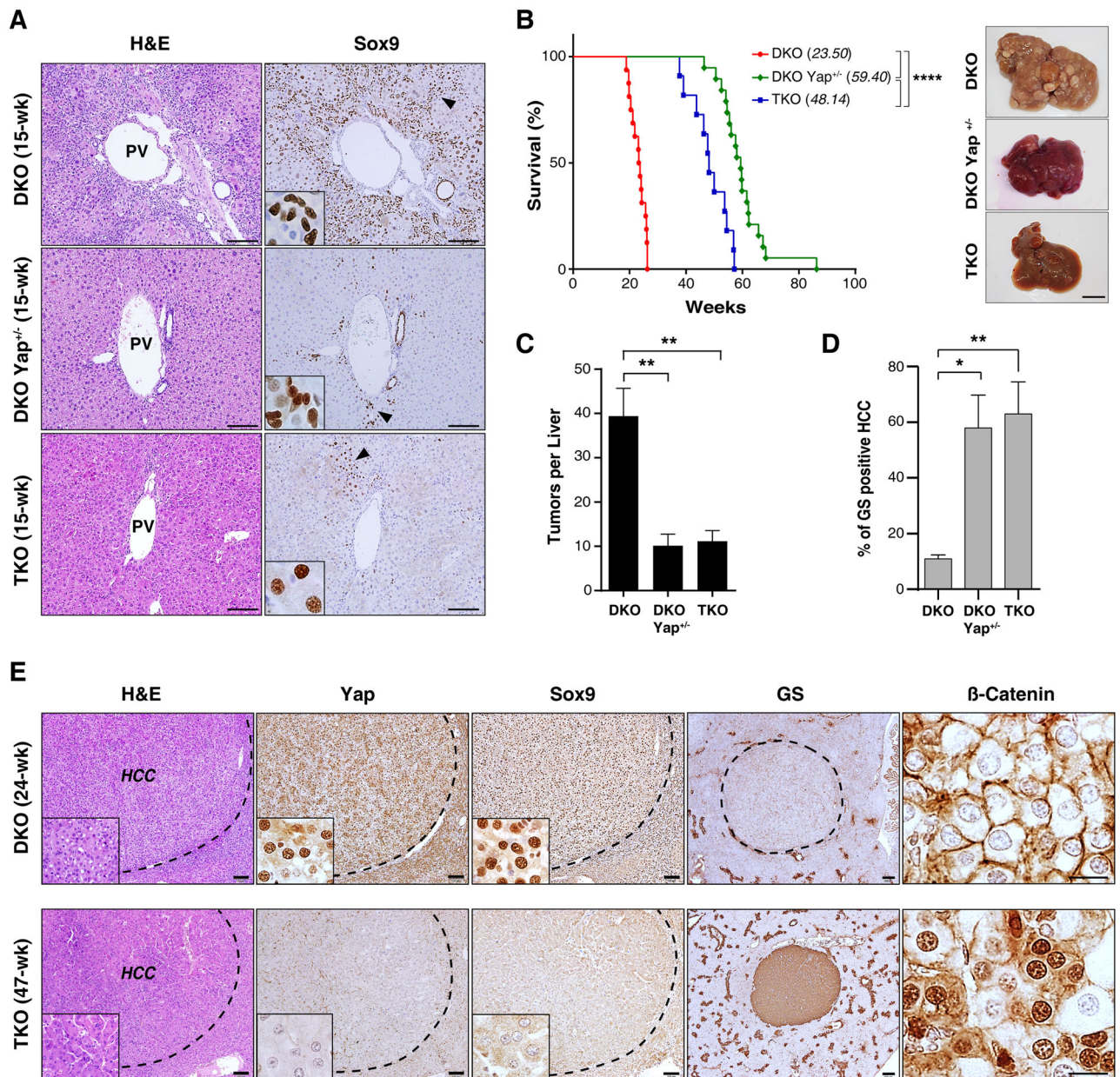


Figure 3. YAP suppresses the β -CATENIN pericentral program and drives invasive HCC downstream of *Mst1/Mst2* DKO

A. Analysis of the indicated genotypes by H&E and SOX9 staining at 15 weeks. The dedifferentiation of hepatocytes to ADCs caused by *Mst1/Mst2* DKO is blocked by hemizygous or homozygous *Yap* deletion, although scattered SOX9-positive cells are observed by this time point. *Insets*: High magnification images of regions denoted by arrowheads in the main panels. Note differences in the morphology of SOX9-positive cells between genotypes. Scale bar: 100 μ m

B. Left panel: Kaplan-Meier analysis showing time until animals reached endpoints for disease burden requiring euthanasia (see **Methods**). Median survival is indicated in brackets.

N= 16 mice (DKO), 19 mice (DKO Yap^{+/-}), 11 (TKO). ****p<0.0001. *Right panels*: Gross images of representative livers at sacrifice.

C. Mean tumor burden at sacrifice. N= 8 mice (DKO), 7 mice (DKO Yap^{+/-}) and 7 mice (TKO). Error bars indicate S.E.M. **p<0.01.

D, E. Histologic and IHC analysis of tumors from DKO and TKO mice with end-stage disease. GS staining is quantified in **(D)**. N= 4 mice per group. Error bars indicate S.E.M.*p<0.05 and **p<0.01. All tumors showed HCC histopathology, although distinct staining patterns were noted for liver markers. DKO tumors **(E, top)** stained positive for SOX9 and negative for GS and nuclear β -catenin, whereas the majority of TKO tumors **(E, bottom)** showed the opposite pattern. All TKO tumors lacked YAP staining. Scale bars: 20 μ m (β -catenin), 100 μ m (H&E, YAP, SOX9) and 200 μ m (GS). See also Figure S3.

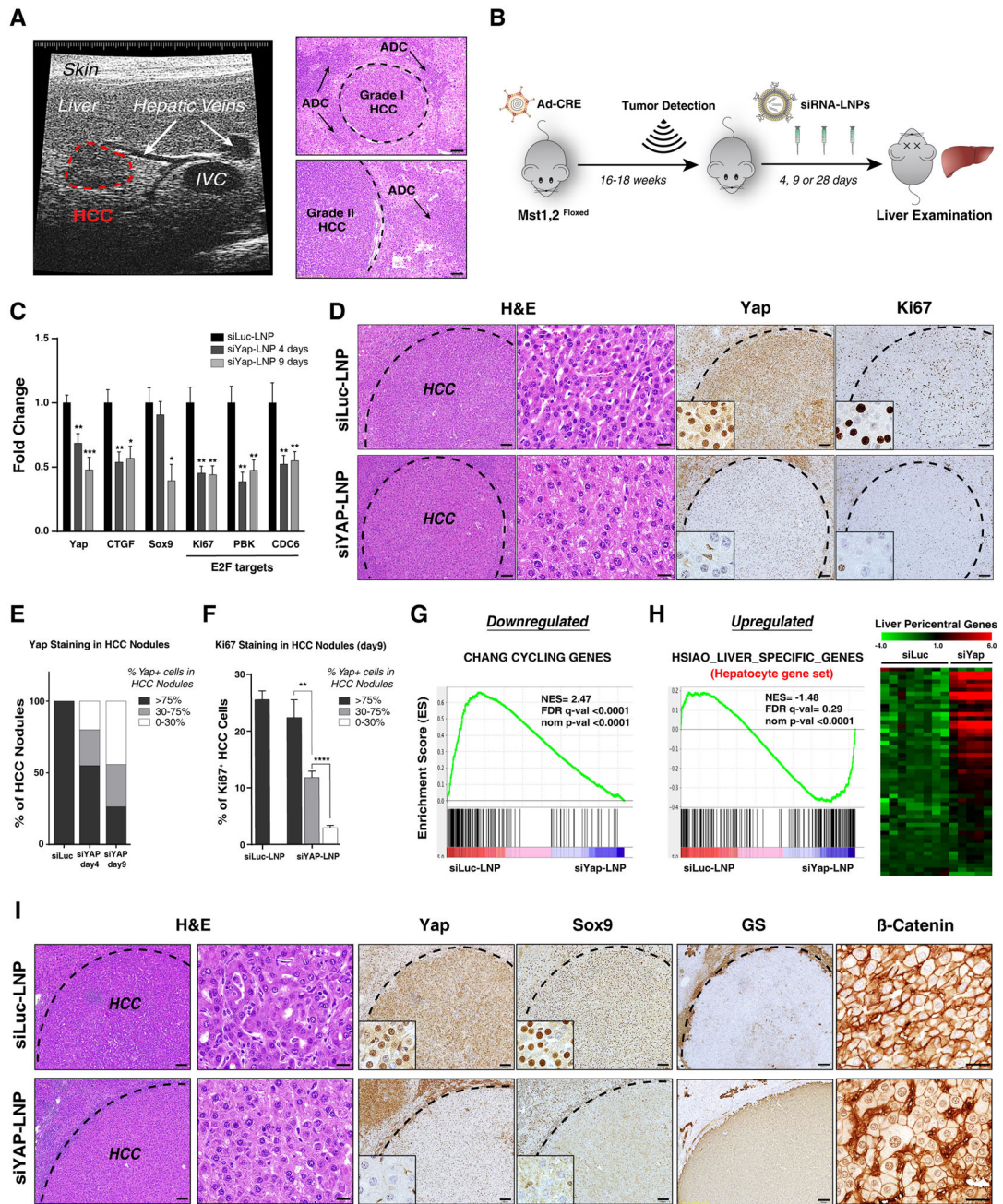


Figure 4. siLNP-mediated YAP silencing induces proliferative arrest and a pericentral hepatocyte differentiation program in advanced HCC

A. Ultrasound (US) detection of a liver tumor in DKO^{Ad} at 16 weeks after Adeno-Cre injection. The right panel shows corresponding histology of liver tumors. Interior vena cava (IVC). Scale bar: 100 μ m.

B. Schematic of therapeutic study. Upon detection of tumors by US imaging, animals were randomized into groups receiving siYAP-LNPs or control siLuc-LNPs and euthanized at the indicated time points.

C. qRT-PCR analysis of tumors isolated after 4 or 9 days treatment. N= 32 tumors (siLuc), 18 tumors (siYAP 4 days) and 16 tumors (siYAP 9 days). Error bars indicate S.E.M. * $p < 0.05$, ** $p < 0.01$, *** $p < 0.001$.

D. Representative IHC staining for YAP and KI67 in HCCs following 9 days treatment. Note that at 9 days HCC cells are preferentially targeted by siYAP-LNPs, whereas all liver cells show knockdown at later time points (see Fig. 5C). Scale bars: 20 μm (H&E, *right*) and 100 μm (H&E *left*, YAP, KI67).

E. Quantification of YAP staining in HCC nodules at day 4 and 9. The chart shows the % of HCC nodules containing the indicated proportions of YAP-positive tumor cells (black, >75% of cells YAP-positive; grey, 30–75%; white, 0–30%). Note that YAP knockdown efficiency increases from day 4 to day 9.

F. Quantification of KI67 staining at day 9. The chart shows % KI67-positive HCC cells in different tumor nodules grouped according to degree of YAP knockdown. Note that the decrease in KI67 staining correlates with effectiveness of YAP knockdown. siLuc-LNP: N= 20 tumors, from 3 treated mice; siYAP-LNP: N= 34 tumors from 4 treated mice. Error bars indicate S.E.M. ** $p < 0.01$, **** $p < 0.0001$.

G, H. GSEA of differentially expressed genes in response to siYAP-LNPs versus control siLuc-LNPs (day 9). **G.** Cell cycle genes are repressed. **H.** *Left panel.* Markers of hepatocyte differentiation are induced. *Right panel.* Heat map showing induction of markers specific to pericentral hepatocytes (Braeuning et al., 2006). NES: Normalized enrichment score. FDR: False discovery rate.

I. By day 9, siYAP-LNPs result in loss of SOX9 staining, nuclear translocation of β -CATENIN and induction of GS. Scale bar 20 μm (H&E *right*, β -catenin) and 100 μm (H&E *left*, YAP, SOX9, GS).

See also Figure S4 and Table S2.

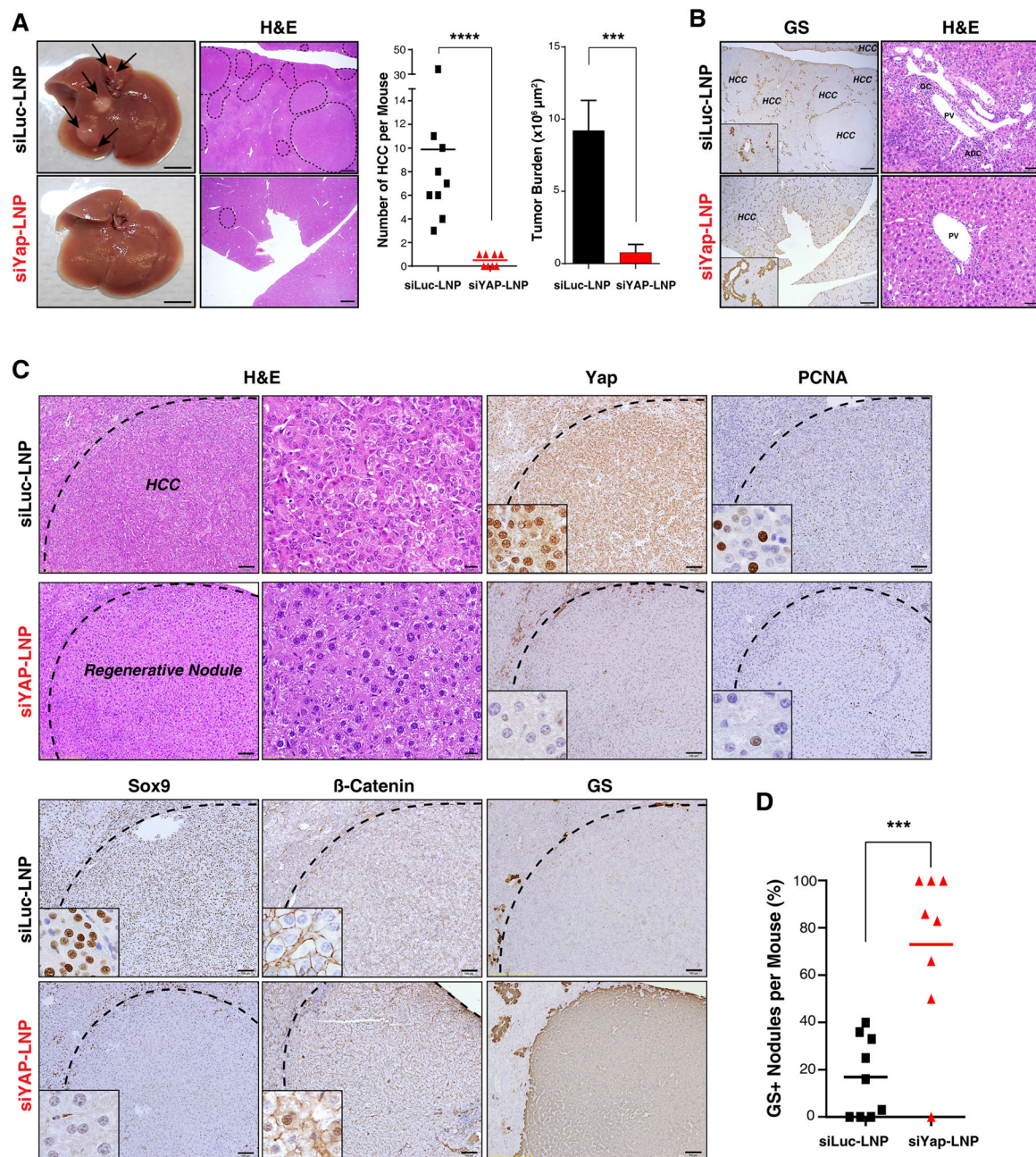


Figure 5. siLNP-mediated YAP silencing is an effective differentiation therapy in advanced HCC Following detection of tumors by US imaging, DKO^{Ad} mice were treated with siRNA-LNPs for 28 days and then euthanized. **A.** Representative gross liver images and H&E stained sections. Arrows: visible liver tumors. Dotted lines: histologically confirmed HCC lesions. The charts show the number of histologically-validated HCC lesions/mouse (*left*) and tumor area occupied per whole liver cross-section (*right*, see **Methods**). N= 9 mice (siLuc-LNP) and 8 mice (siYAP-LNP). Scale bar 5 mm (gross) and 1 mm (H&E). Error bars indicate S.E.M. *** $p < 0.001$, **** $p < 0.0001$. **B.** The liver parenchyma shows restoration of zonal GS expression and disappearance of ADCs upon siYAP-LNP treatment. HCC lesions are

indicated. Scale bar: 1 μm (GS) and 50 μm (H&E) **C.** siYAP-LNP treatment results in replacement of invasive HCCs by benign nodules with histopathologic features consistent with differentiation to regenerative hepatocytes, associated with loss of SOX9, infrequent PCNA staining, focal induction of nuclear β -CATENIN, and strong upregulation of GS. Scale bars: 100 μm and 20 μm (H&E *right panel*). **D.** Chart quantifying the proportion of nodules staining positive for GS. Error bars indicate S.E.M. *** $p < 0.001$. See also Figure S5.

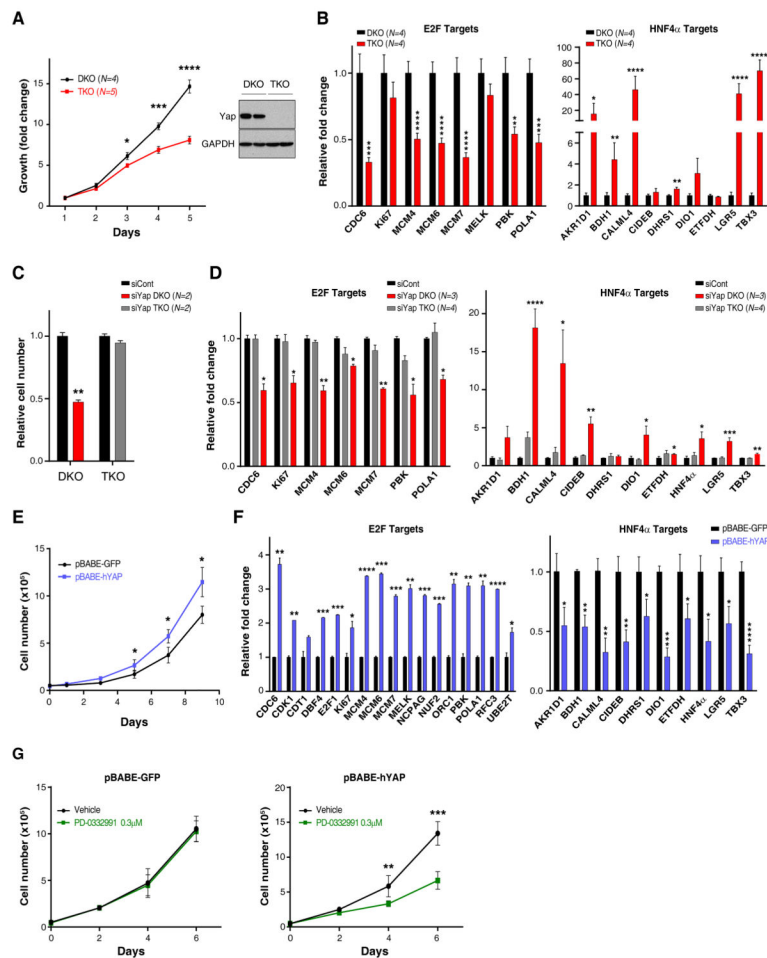


Figure 6. YAP positively regulates an E2F proliferation program and suppresses the Hnf4a hepatocyte differentiation pathway

A. Left panel: Low passage HCC cultures derived from DKO mice display a proliferative advantage compared to TKO lines. N = number of independent cultures tested in each group.

Right panel: Western blot analysis confirming that YAP expression is restricted to the DKO lines. **B.** qRT-PCR analysis shows that DKO lines are characterized by higher basal expression of E2F targets (*left panel*) and lower expression of HNF4a targets (*right panel*). Error bars indicate S.E.M. *p<0.05, **p<0.01, ***p<0.001, ****p<0.0001

C, D. DKO and TKO cell lines were transfected with siRNA against YAP or control siRNA. **C.** Quantification of cell growth data showing that siRNA-mediated YAP knockdown causes proliferative arrest of DKO lines but does not affect TKO cells. **D.** qRT-PCR analysis showing that YAP knockdown in DKO cells results in a significant decrease in the expression of multiple E2F-regulated cell cycle genes (*left panel*) and pronounced activation of HNF4A targets (*right panel*). Error bars indicate S.E.M. *p<0.05, **p<0.01, ***p<0.001, ****p<0.0001.

E–G. TKO cells were transduced with retroviruses expressing human YAP (hYAP) or GFP control. **E.** YAP expression significantly increases the proliferation of TKO cells (*left panel*). **F.** Forced expression of YAP induces E2F targets (*left panel*) and inhibits HNF4A targets (*right panel*). Error bars indicate S.E.M. *p<0.05, **p<0.01, ***p<0.001, ****p<0.0001. **G.**

Treatment with a CDK4/6 inhibitor (PD-0332991, 0.3 μ M) impairs proliferation of TKO cells expressing YAP (*right panel*), without affecting GFP-expressing TKO control cells (*left panel*). Error bars indicate S.E.M. ** $p < 0.01$, *** $p < 0.001$. See also Figure S6.

Author Manuscript

Author Manuscript

Author Manuscript

Author Manuscript

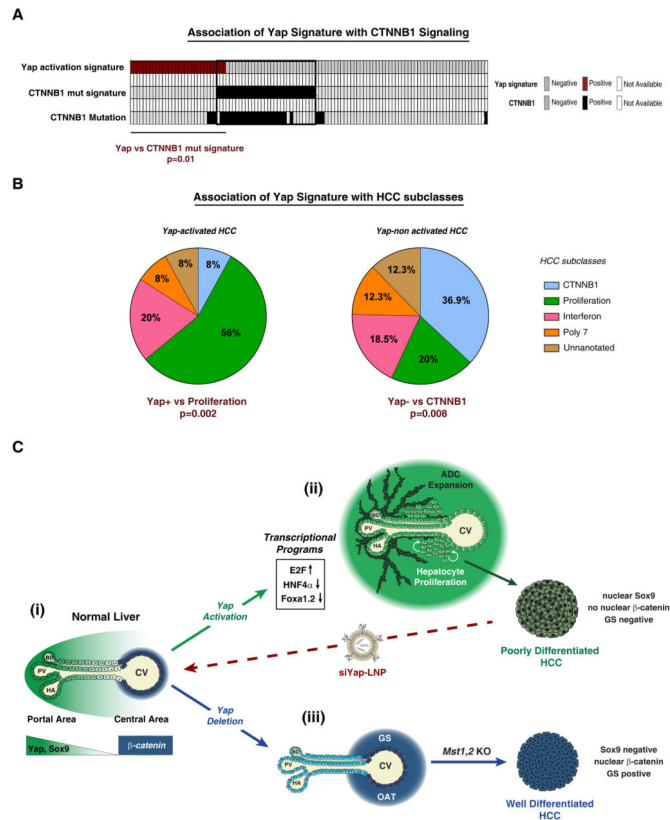


Figure 7. The YAP activity signature is enriched in human HCC subtypes defined by lack of CTNNB1 mutation and a proliferation gene profile

A. Analysis of 111 human HCC specimens reveals inverse correlation between the *CTNNB1*-mutation signature and a YAP activation signature. **B.** Using a second HCC classification system (Chiang et al., 2008), the YAP activation signature (YAP+) is positively correlated with the aggressive Proliferation subclass, whereas absence of the signature (YAP-) significantly correlates with the *CTNNB1* subclass. Fisher's exact test was used for statistical analysis. **C.** Model illustrating the impact of Hippo/YAP modulation on liver biology. (i) In normal liver, YAP shows a decreasing gradient of nuclear and cytoplasmic expression along the porto-central axis. The final layer of hepatocytes adjacent to the central vein completely lacks YAP expression, whereas active β -catenin and GS are restricted to these cells. (ii) Activation of YAP in hepatocytes results in induction of proliferation-related E2F target genes, downregulation of the targets of the HNF4A and FOXA1,2, and loss of pericentral β -CATENIN targets (e.g. GS, OAT), as well as hepatocyte proliferation throughout the lobule and dedifferentiation of hepatocytes to ADCs in the portal area. The resulting HCCs are poorly differentiated, express SOX9 and lack nuclear β -CATENIN and its target, GS. Treatment with siYAP-LNPs leads to tumor regression and hepatocyte differentiation. (iii) Yap deletion leads to an expansion of β -CATENIN targets in the central area. Additionally, Yap ablation completely blocks hepatocyte proliferation and oval cell expansion resulting from *Mst1/Mst2* loss, and delays HCC development. The HCCs that develop display distinct differentiation markers and histopathology as compared to Yap-driven HCCs.

ADC: Atypical Ductal Cells, BD: Bile duct, CV: Central vein, GS: glutamine synthetase, HA: Hepatic artery, OAT: ornithine aminotransferase, PV: Portal vein. See also Figure S7.

Author Manuscript

Author Manuscript

Author Manuscript

Author Manuscript